CLASTRE, J. & GAY, R. (1950*a*). *C. R. Acad. Sci., Paris*, **230**, 1976.
CLASTRE, J. & GAY, R. (1950*b*). *J. Phys. Radium*, **11**, 75.
COCHRAN, W. (1954). *Acta Cryst.* **7**, 581.
COCHRAN, W. & PENFOLD, B. R. (1952). *Acta Cryst.* **5**, 644.
HAUPTMAN, H. & KARLE, J. (1950). *Acta Cryst.* **3**, 478.
HAUPTMAN, H. & KARLE, J. (1957). *Acta Cryst.* **10**, 267.
KARLE, J. & HAUPTMAN, H. (1957). *Acta Cryst.* **10**, 515.
KLUG, A. (1958). *Acta Cryst.* **11**, 515.
SAYRE, D. (1952). *Acta Cryst.* **5**, 60.
WOOLFSON, M. M. (1958). *Acta Cryst.* **11**, 277.
WRINCH, D. (1939). *Phil. Mag.* **27**, 98.

Acta Cryst. (1958). **11**, 585

Extinction Effects in Neutron Scattering from Single Magnetic Crystals*

BY WALTER C. HAMILTON

Chemistry Department, Brookhaven National Laboratory, Upton, Long Island, New York, U.S.A.

(*Received* 2 *December* 1957)

Results arising from the treatment of magnetic scattering of neutrons, taking due account of the possibility of polarization of the neutron beam, indicate that the usual expressions for primary and secondary extinction must be modified in certain cases. Extinction, particularly primary extinction, will be generally more severe for reflections which have both nuclear and magnetic contributions than for either pure nuclear or pure magnetic reflections. Formulas and curves are presented for primary and secondary extinction corrections which are applicable to both magnetized and unmagnetized ferromagnetic or antiferromagnetic crystals. Some of the results obtained may be conveniently used to determine relative amounts of primary and secondary extinction, and consequently both mosaic block size and angular distribution. Many of the calculations are of interest in predicting the effects of extinction on experiments designed either to produce or use polarized neutron beams.

The precession of the neutron polarization axis about the magnetic axis can affect the reflected intensity if extinction is severe. This effect is discussed briefly and is shown to be serious only for magnetized crystals.

The appendix discusses the necessary changes in the scattering formulas if all the spins in the unit cell do not lie along a unique magnetic axis.

Introduction

In a recent paper (Hamilton, 1957) the author has discussed secondary extinction corrections for crystals of arbitrary geometrical cross-section. In the example which was chosen to illustrate some of the points discussed in that paper—a synthetic single crystal of magnetite which showed particularly severe extinction—it was noted that several of the reflections which had large magnetic contributions did not give as good a fit to the extinction curves as did the pure nuclear reflections. An empirical extinction curve was found to give a satisfactory fit to the observed intensities of the nuclear reflections, but the intensities of many of the mixed reflections were considerably lower than this curve would predict. This lowered intensity could not be accounted for by any reasonable changes in the parameters describing the magnetic structure, nor in the form factor and saturation curves. Preliminary considerations indicated that this behavior could be explained by a combination of polarization and extinction effects, and the present paper is a detailed elaboration of that point of view.

Following Halpern & Johnson (1939), we may write the wave function for the incident neutron beam as

$$\psi_0 = (2\pi M_0/hk)^{\frac{1}{2}} \exp\,[i\mathbf{k}.\mathbf{r}]\chi_s\,, \qquad (1)$$

where $\mathbf{k}$ is the wave vector $2\pi\mathbf{P}/h$ with $\mathbf{P}$ the neutron momentum, $\mathbf{r}$ is a position vector, M_0 is the neutron mass, and χ_s is the neutron spin function. The scattered wave from a single oriented magnetic ion may then be represented by

$$\psi_H = (2\pi M_0/hk)^{\frac{1}{2}} r^{-1} \exp\,[ikr](b+p\mathbf{q}.\mathbf{s})\chi_s\,, \qquad (2)$$

provided that there is no change in the spin state of the scattering ion. The nuclear and magnetic scattering amplitudes are given by b and p respectively with p defined as

$$p = (e^2\gamma_n S/mc^2)f\,. \qquad (3)$$

Here γ_n is the neutron magnetic moment in nuclear magnetons, S is the spin of the scattering ion, m is the mass of the electron, f is a form factor, and c and e

* Research performed under the auspices of the U.S. Atomic Energy Commission.

have the usual meanings. The spin operator **s** has the following properties:

$$\left.\begin{aligned} \mathbf{s}_x\alpha &= (1/2)\beta, \quad \mathbf{s}_y\alpha = \quad (i/2)\beta, \quad \mathbf{s}_z\alpha = \quad (1/2)\alpha\ , \\ \mathbf{s}_x\beta &= (1/2)\alpha, \quad \mathbf{s}_y\beta = -(i/2)\alpha, \quad \mathbf{s}_z\beta = -(1/2)\beta\ , \end{aligned}\right\} \tag{4}$$

where α and β are the eigenfunctions of $\mathbf{s}_z$. Note that any spin function may be described as

$$\chi_s = a\alpha + b\beta \tag{5}$$

with complex a and b such that χ_s is normalized:

$$|a|^2 + |b|^2 = 1\ . \tag{6}$$

No generality is lost by taking a to be real, and we shall do so. The polarization direction corresponding to χ_s is defined by the polar angles θ_s and φ_s satisfying

$$\cot\left(\tfrac{1}{2}\theta_s\right) = |a|/|b|\ , \tag{7}$$

$$\tan\varphi_s = (b - b^*)/i(b + b^*)\ . \tag{8}$$

Note that we may also write

$$\cos\theta_s = |a|^2 - |b|^2 \equiv P\ , \tag{9}$$

where P is defined as the *polarization* (relative to the z axis). This may also be written as

$$P = (I_\alpha - I_\beta)/(I_\alpha + I_\beta)\ , \tag{10}$$

where I_α and I_β are the intensities of the two beam components with polarization directions corresponding to α and β. The magnetic interaction vector **q** is defined by

$$\mathbf{q} = \boldsymbol{\varepsilon}(\boldsymbol{\varepsilon}.\mathbf{K}) - \mathbf{K}\ , \tag{11}$$

where $\boldsymbol{\varepsilon}$, the scattering vector, is a unit vector perpendicular to the scattering plane and **K** is a unit vector in the ionic spin direction, i.e., the magnetization direction. Note that **q** lies in the plane of $\boldsymbol{\varepsilon}$ and **K**, and is orthogonal to $\boldsymbol{\varepsilon}$. The magnitude of **q** is given by

$$q^2 = \sin^2\tau\ , \tag{12}$$

where τ is the angle between $\boldsymbol{\varepsilon}$ and **K**.

Equation (2) and the following equations may also be interpreted as applying to a structure containing many magnetic ions provided that **q** remains the same or only changes sign for all ions, i.e., the ionic spins are all parallel or antiparallel to a given axis **K**.† This is the situation which presumably obtains in most ferromagnetic and antiferromagnetic materials. In this case, b may be replaced by the nuclear structure factor

$$N = \sum_j b_j \exp\left[i\mathbf{r}_j.\mathbf{h}\right]‡ \tag{13}$$

and p by the magnetic structure factor

$$M = \sum_j (\pm p_j) \exp\left[i\mathbf{r}_j.\mathbf{h}\right]\ , \tag{14}$$

p_j being given an negative sign if the spin of the jth ion is antiparallel to the unique **K**, positive if parallel. The formulas for the scattering are more complex if the ionic spins do not have a unique axis within a single domain; this situation will be discussed in the Appendix.

The cross-section for scattering from a spin direction χ_s into a spin direction χ_s' is

$$\sigma_{\chi_s \to \chi_{s'}} = \left|(\chi_s|N + 2M\mathbf{q}.\mathbf{s}|\chi_s')\right|^2\ . \tag{15}$$

The total scattering cross-section for an incident beam with spin function χ_s is obtained by summing over the spin of the scattered wave

$$\sigma_{\chi_s} = \sum_{\chi_s'} \left|(\chi_s|N + 2M\mathbf{q}.\mathbf{s}|\chi_s')\right|^2\ .* \tag{16}$$

Any unpolarized neutron beam may be regarded as a superposition in equal amounts of two beams with polarization characterized by the functions α and β relative to an arbitrary z axis. If we consider an incident beam which is composed entirely of the α component, we may write the total scattering cross-section for this beam as

$$\sigma_\alpha = \left|(\alpha|N + 2M\mathbf{q}.\mathbf{s}|\alpha)\right|^2 + \left|(\alpha|N + 2M\mathbf{q}.\mathbf{s}|\beta)\right|^2 \tag{17}$$

$$= N^2 + q^2M^2 + 2NMq_z \tag{18}$$

since the following relations are true:

$$(\alpha|\mathbf{q}.\mathbf{s}|\alpha)^2 + (\alpha|\mathbf{q}.\mathbf{s}|\beta)^2 = \tfrac{1}{4}q^2\ , \tag{19}$$

$$(\alpha|\mathbf{q}.\mathbf{s}|\alpha) = \tfrac{1}{2}q_z\ . \tag{20}$$

Similarly we find

$$\sigma_\beta = N^2 + q^2M^2 - 2NMq_z\ . \tag{21}$$

Primary extinction

It has been shown by Goldberger & Seitz (1947) that the equations for the dynamical interaction of neutrons are formally the same as those for X-rays (Zachariasen, 1945, § III). Although the treatment of Goldberger & Seitz is applied only to pure nuclear reflections, it may be extended to magnetic and mixed reflections by replacing the nuclear scattering cross-section by the combined cross-section involving the nuclear magnetic interaction. The magnetic scattering potential may be treated formally as being of the same type as a nuclear scattering potential with a form factor.

In the following, we shall make frequent use of the quantity

$$A = \lambda t_0 |F|/V_c(\gamma_0\gamma_H)^{\frac{1}{2}}\ , \tag{22}$$

† Parallel and antiparallel **q** can also be obtained if $\mathbf{K}_1$ and $\mathbf{K}_2$ make the same angle (not necessarily 90°) with $\boldsymbol{\varepsilon}$ and if $\boldsymbol{\varepsilon}$, $\mathbf{K}_1$, and $\mathbf{K}_2$ are coplanar. This is a rather special situation unlikely to be met with in practice.

‡ The reciprocal-lattice vector $2\pi(h\mathbf{a}^* + k\mathbf{b}^* + l\mathbf{c}^*)$ has been denoted **h** rather than the usual **s** to avoid confusion with the spin operator **s**. **h** is equal to $2\pi d^*\boldsymbol{\varepsilon}$.

* Summation over the two states, α and β, is equivalent to integration over θ and φ.

where $|F|$ will be defined as $\sigma^{\frac{1}{2}}$, λ is the neutron wave length, t_0 is the thickness of the perfect crystal being considered, V_c is the unit-cell volume, and γ_O and γ_H are the direction cosines of the incident and diffracted beams relative to the normal to the crystal face. This value of A may be inserted into the equations given by Zachariasen (1945) to determine the diffracted intensities in the presence of primary extinction. However, in order to apply the equations correctly, we must treat each direction of polarization separately, as the scattering cross-section and hence A depend on the polarization of the incident beam; the resultant intensities are then added. Furthermore, the equations can be applied in the usual form only if the polarized beam under investigation retains the same direction of polarization after all scattering processes, i.e., the axis along which the spin is analyzed must be such as to make the second term in (17) equal to zero:*

$$(\alpha|\mathbf{q}.\mathbf{s}|\beta)^2 = 0 . \tag{23}$$

This equation implies the following condition:

$$q_x = q_y = 0 \quad \text{and} \quad q_z = q , \tag{24}$$

i.e., the spin must be analyzed along the direction of $\mathbf{q}$. Equations (18) and (21) then reduce to

$$\left.\begin{aligned} \sigma_\alpha &= N^2+2MNq+M^2q^2 , \\ \sigma_\beta &= N^2-2MNq+M^2q^2 , \end{aligned}\right\} \tag{25}$$

or

$$\left.\begin{aligned} \sigma_\alpha^{\frac{1}{2}} \equiv |F_+| &= |N+Mq| , \\ \sigma_\beta^{\frac{1}{2}} \equiv |F_-| &= |N-Mq| . \end{aligned}\right\} \tag{26}$$

We shall now examine the results of inserting these values for $|F|$ into the equations given by Zachariasen (1945). We shall for simplicity in the following development assume that the absorption cross-section is much smaller than the scattering cross-section and may hence be neglected. This is an adequate approximation for many neutron diffraction problems of current interest. It shall furthermore be assumed that the coherently scattering crystal block under consideration is a single magnetic domain.†

The equations for the dynamical theory have been solved only for infinite flat plates, and it is necessary to distinguish two cases: the *Laue case*, in which the diffracted beam emerges from the side of the plate opposite the entry face, and the *Bragg case*, in which it emerges from the same side. It may be noted here that for the symmetrical diffraction condition defined by

$$\gamma_O = \gamma_H$$

the factor $(\gamma_O\gamma_H)^{\frac{1}{2}}$ is equal to $\sin\theta_B$ or $\cos\theta_B$ for the Bragg or Laue case, respectively. We shall consider in detail only the equations for the symmetrical Bragg case.* The integrated intensity for the rotating crystal method is given by

$$\begin{aligned} R^\theta &= \frac{\lambda^2|F|\tanh A}{V_c \sin 2\theta_B} \\ &\equiv k_1k_2|F|\tanh(k_1|F|) \end{aligned} \tag{27}$$

with

$$k_1 = \lambda t_0/V_c \sin\theta_B , \tag{28}$$

$$k_2 = \lambda/2t_0 \cos\theta_B . \tag{29}$$

The following limiting conditions are important:

$$R^\theta \approx k_1^2k_2|F|^2 \quad \text{if} \quad k_1|F| \ll 1 , \tag{30}$$

$$R^\theta \approx k_1k_2|F| \quad \text{if} \quad k_1|F| \gg 1 . \tag{31}$$

We obtain then for the integrated intensities of the two polarized components

$$R_+^\theta = k_1k_2|F_+|\tanh(k_1|F_+|) , \tag{32}$$

$$R_-^\theta = k_1k_2|F_-|\tanh(k_1|F_-|) .\dagger \tag{33}$$

If the incident polarization is given by

$$P_0 = (1-R)/(1+R) \quad \text{with} \quad R = I^\beta/I^\alpha , \tag{34}$$

the primary extinction ratio E_p, defined as the actual integrated intensity divided by the ideal integrated intensity for a 'thin' crystal (30), is found to be

$$E_p = \frac{|F_+|\tanh(k_1|F_+|)+R|F_-|\tanh(k_1|F_-|)}{k_1(|F_+|^2+R|F_-|^2)} . \tag{35}$$

The values of E_p for an initially unpolarized beam ($R = 1$) have been calculated and are plotted in Fig. 1 against

$$k_1\langle F^2\rangle^{\frac{1}{2}} \equiv \{\tfrac{1}{2}k_1^2(|F_+|^2+|F_-|^2)\}^{\frac{1}{2}} \tag{36}$$

for several values of $|F_-|/|F_+|$.‡ The most interesting feature of these curves is the dependence on the ratio $|F_-|/|F_+|$. It is clearly seen that extinction affects the mixed magnetic and nuclear reflections considerably more than the pure nuclear or pure magnetic reflec-

* It would be interesting to carry through the theory of dynamical scattering for cases where spin flip is allowed, thus considering a set of four coupled waves rather than two. Such a treatment is necessary, however, only if the ionic spins are not all parallel or anti-parallel to a unique direction, and even then only in non-centrosymmetric structures (see Appendix).

† The domains in a mosaic crystal may well be *larger* than the mosaic blocks. Our assumption, which seems plausible, is that they are in any case no smaller.

* The equations for the Laue case are identical to those for the Bragg case if $\tanh A$ in the expressions below is replaced by

$$\tfrac{1}{2}\int_0^{2A} J_0(\varrho)d\varrho \equiv \sum_{n=0}^{\infty} J_{2n+1}(2A) ,$$

where J_n is the Bessel function of order n, and if the appropriate value for $(\gamma_O\gamma_H)^{\frac{1}{2}}$ is used in the definition of A.

† Chandrasekhar & Weiss (1957) have recently tabulated the ratio R_-^θ/R_+^θ as a function of A and M/N in the approximation that $A\tanh A \approx A^2-\frac{1}{3}A^4$.

‡ Note that $|F_-|/|F_+|$ is equal to 1 for pure nuclear or pure magnetic reflections.

tions. The minimum value of the extinction ratio is reached for $|F_-| = 0$, i.e. for $N = Mq$.

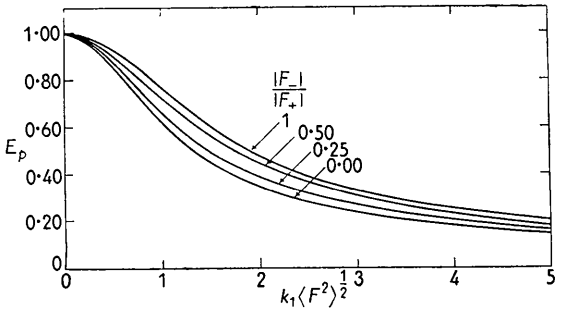

Fig. 1. Primary extinction ratio E_p versus $k_1\langle F^2\rangle^{\frac{1}{2}} = \{\frac{1}{2}k_1^2(|F_+|^2+|F_-|^2)\}^{\frac{1}{2}}$. Bragg diffraction of unpolarized incident beam from perfect crystal plate. Curves are shown for several values of $|F_-|/|F_+| = |N-Mq|/|N+Mq|$.

It is interesting also to examine the effect of the extinction on the polarization of the diffracted beam. If the incident beam has a polarization given by P_0, the diffracted beam will have a polarization

$$P = \frac{(R_+^\theta - R_-^\theta)+P_0(R_+^\theta+R_-^\theta)}{(R_+^\theta+R_-^\theta)+P_0(R_+^\theta-R_-^\theta)} . \tag{37}$$

Only if R_+^θ is equal to R_-^θ (pure nuclear or pure magnetic reflection) is the polarization unchanged. In Fig. 2 are plotted values of P against $k_1\langle F^2\rangle^{\frac{1}{2}}$ for

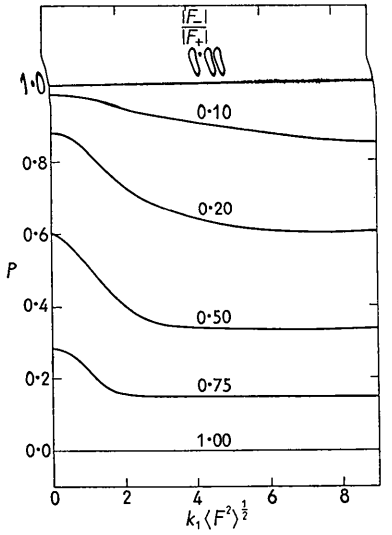

Fig. 2. Polarization of diffracted beam versus $k_1\langle F^2\rangle^{\frac{1}{2}}$. Same diffraction conditions as those for Fig. 1.

an initially unpolarized beam. The limiting values are, of course, for low intensities:

$$P = \frac{|F_+|^2-|F_-|^2}{|F_+|^2+|F_-|^2} , \tag{38}$$

and for high intensities:

$$P = \frac{|F_+|-|F_-|}{|F_+|+|F_-|} . \tag{39}$$

The extinction curves for the Laue case are similar to those for the Bragg case with the exceptions that the limiting intensities are one-half as large and that the curves of R^θ against $|F|$ do not rise smoothly but fluctuate about the limiting value.* These fluctuations are largely smoothed out if one is dealing with a mosaic crystal where an average must be made over a distribution of mosaic block thicknesses. As neither the Laue nor the Bragg case would seem to adequately describe the situation obtaining in a real crystal, we present here only the results for the Bragg case, as these should provide a qualitative picture of the true situation. Under actual experimental conditions, we probably have an approximately cubic crystallite completely immersed in the X-ray or neutron beam rather than the idealized infinite flat plates on which a smaller beam falls. There is a real need for a treatment of the dynamical theory of diffraction for more realistically shaped crystals. It is the author's viewpoint that the values for the intensity would be intermediate between the Bragg case and a smoothed Laue case and that the extinction function for either case would give a satisfactory fit to experimental data, but with a suitable—and as yet unknown—redefinition of scale parameter. That is, the meaning of $t_0(\gamma_0\gamma_H)^{-\frac{1}{2}}$ —the average path length—in (22) would depend on the size and *shape* of the crystal rather than on the diffraction angle and single dimension alone.

Secondary extinction

(a) *General consideration*

In essentially all cases of practical interest, we will not be dealing with a single, coherently-scattering block for which the treatment in the preceding section is adequate. Rather, we must consider a real crystal as being composed of many individual mosaic blocks, each of which will have a reflectivity governed by the considerations of the dynamical theory discussed in the preceding section. We must distinguish two situations, characterized by whether the crystal as a whole has a unique axis of magnetization or not, not only because of the difference in the average value of q^2 but because of the effect of beam polarization on the interaction of the various extinction effects.

A review of a few of the developments regarding secondary extinction may be in order here (see Hamilton, 1957 and Zachariasen, 1945). It is convenient to define the reflectivity as

$$\sigma'' = Q'W(\Delta\theta) , \tag{40}$$

where $W(\Delta\theta)$ is a distribution function characterizing the mosaic structure of the crystal, and Q' is defined as

$$Q' = QE_p , \tag{41}$$

* See Zachariasen, 1945, p. 134, for a graph of this curve.

with E_p being the primary extinction correction and with Q defined as follows:

$$Q = \lambda^3 F^2/V_c^2 \sin 2\theta_B . \tag{42}$$

for neutrons, and

$$Q = e^4(1+\cos^2 2\theta)\lambda^3 F^2/2m^2c^4V_c^2 \sin 2\theta_B \tag{43}$$

for X-rays. One may then write differential equations for the power in the incident and diffracted beams in terms of $\sigma''dn$ and $\sigma''dm$ (and μdn and μdm as well if absorption is important) where dn and dm are elements of length parallel to the incident and diffracted beams. The integrated diffracted intensity is obtained by integrating the power in the diffracted beam over the exit surface of the crystal and over the mosaic distribution parameter $\Delta\theta$. For plane parallel crystal plates, we have

$$\left.\begin{aligned} \sigma''dn &= \sigma''dt/\gamma_O , \\ \sigma''dm &= \sigma''dt/\gamma_H , \end{aligned}\right\} \tag{44}$$

where dt is an element of length normal to the plate, and consequently in treatments confined to such cases (Zachariasen, 1945), the reflectivity can be defined as

$$\sigma_H = \sigma''/\gamma_H \tag{45}$$

for the diffracted beam and

$$\sigma_O = \sigma''/\gamma_O \tag{46}$$

for the incident beam. For the symmetrical diffraction condition, σ_O is equal to σ_H. We shall for the most part use the definition in (40) for the reflectivity, but will also have some occasion to use σ as defined in (45) and (46).

(*b*) *Magnetized mosaic crystal*

If the crystal under consideration is magnetized, i.e. has all its domains parallel, the value of q will be the same for all mosaic blocks. We may then carry out the secondary extinction calculations in the usual way* for each polarized component alone and add the results at the end. For the Bragg case† we may thus write

$$Q'_+ = Q_+ \tanh (k_1|F_+|)/k_1|F_+| , \tag{47}$$

$$Q'_- = Q_- \tanh (k_1|F_-|)/k_1|F_-| , \tag{48}$$

where Q_+ and Q_- are defined as in (42) with the appropriate values for F^2. R^θ_+ and R^θ_- are then calculated for each of the Q', and the total extinction ratio (for an unpolarized incident beam) is given by

$$E_pE_s = \frac{(R^\theta_+ + R^\theta_-)}{(Q_+ + Q_-)V\mathscr{A}} , \tag{49}$$

where V is the volume of the crystal, and $\mathscr{A}$ is a pure absorption correction. The secondary extinction ratio alone is of course

$$E_s = \frac{(R^\theta_+ + R^\theta_-)}{(Q'_+ + Q'_-)V\mathscr{A}} . \tag{50}$$

It is easily seen from (50) that, in this case, secondary extinction, even in the absence of primary extinction, can lead to a higher degree of extinction for mixed reflections than for pure nuclear or pure magnetic reflections.

(*c*) *Unmagnetized mosaic crystal: random domains*

If the crystal is not magnetized, the vectors **K** and **q** will vary from one mosaic block to another. Consequently we must calculate an $(E_p)_i$ and a corresponding σ_i'' for each block.* Although the scattering in each mosaic block gives rise to a polarization of the scattered beam, it is clear that the average polarization at any depth in the crystal, and hence striking any layer of mosaic blocks, is zero, for in the ideal unmagnetized crystal there are as many domains with magnetic axes antiparallel as parallel to a given direction. We may then average σ_i'' over all values of **K** and the two directions of polarization to obtain an average $\overline{R^\theta}$ and a corresponding $\overline{E_p}$ for the whole crystal. Using this $\overline{E_p}$, we go through the secondary-extinction calculation in the usual way.

If the crystal possesses unique axes of magnetization, these define the **K**'s over which the average must be taken. For the purposes of illustration, we will consider a hypothetical case in which the direction of **K** is assumed to be random, and hence all values of **q** in the plane perpendicular to **ε** are equally probable. Then we have

$$\overline{R^\theta} = \tfrac{1}{4}k_1k_2\int_0^\pi |N+M\sin\tau|\tanh(k_1|N+M\sin\tau|)\sin\tau\, d\tau + \tfrac{1}{4}k_1k_2\int_0^\pi |N-M\sin\tau|\tanh(k_1|N-M\sin\tau|)\sin\tau\, d\tau \tag{51}$$

and

$$\overline{E_p} = \overline{R^\theta}/k_1^2k_2(N^2+2M^2/3) . \tag{52}$$

This quantity has been calculated for several values

* See Zachariasen (1945) for the treatment of infinite flat plates and Hamilton (1957) for the extension to crystals of arbitrary shape.

† Bragg case here refers only to the diffraction from the individual mosaic block and not necessarily to the crystal *in toto*. This is, we may take the ideal Bragg case as an approximation to the primary-extinction conditions and apply the results to an arbitrarily shaped crystal in the secondary-extinction calculation. For a real crystal, k_1 should perhaps be defined as proportional to a mean thickness rather than to $t_0/\sin\theta$.

* There may possibly be more than one mosaic block in each domain so that some neighboring blocks will have identical σ_i''. However, the treatment in this section is not valid if the domains are so much larger than the mosaic blocks that there is appreciable secondary extinction in a single domain. For such a case, the treatments in this and the preceding section must be combined. That is, each domain should be treated as a single magnetized mosaic crystal and an average then taken over all domains.

of N/M. Fig. 3 is a plot of $\overline{E_p}$ against the value of E_p for a pure nuclear peak of the same ideal calculated intensity, i.e.,

$$E_p(N/M = \infty) = \tanh (k_1|F|)/k_1|F| \,. \qquad (53)$$

The same values are plotted in a perhaps more useful way in Fig. 4. The ratio of $\overline{E_p}$ to E_p for a pure nuclear peak is plotted against the ratio N/M, and curves are given for several values of $E_p(N/M = \infty)$. Here again, we see that reflections with magnetic contributions are more seriously affected by primary extinction. There is, however, no difference in the way magnetic and nuclear reflections are affected by *secondary* extinction for this case of the unmagnetized crystal. We have thus an interesting method for determining independently the amounts of primary and secondary extinction and, consequently, both the mosaic-spread parameter and the average size of the mosaic blocks. If a crystal exhibits secondary extinction only, all reflections (for a small range of Bragg angles) can be fitted to the same secondary-extinction curve. If, however, we plot I_O against I_C for a crystal which exhibits primary extinction as well, we will find that a smooth curve can be drawn through the points representing the pure nuclear reflections, but that the points representing reflections with magnetic contributions will lie below this curve.* The ratio of the calculated intensity estimated from the curve to the actual calculated intensity is equal to the ratio of the primary extinction coefficients: $E_p(N/M)/E_p(\infty)$. From this ratio and the known value of N/M, we may find from the curves in Figs. 3 and 4 the actual primary extinction coefficient and hence the value of k_1 and t_0. Knowing these, we can calculate the amount of primary extinction for each reflection and, by difference, the amount of secondary extinction and η, the mosaic-spread parameter.

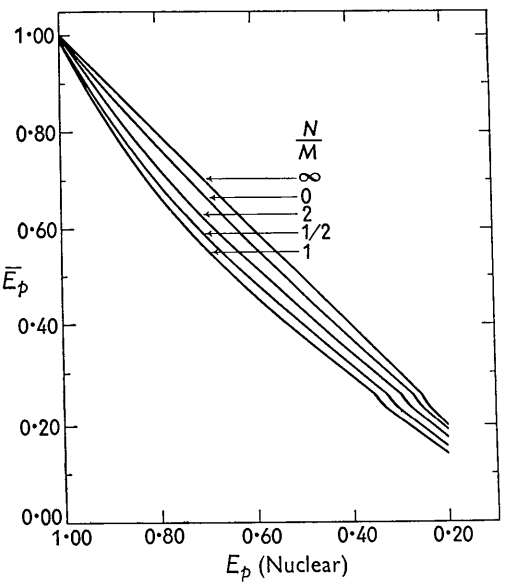

Fig. 3. Mean primary extinction ratio $\overline{E_p}$ for mixed reflections versus $\overline{E_p}$ for pure nuclear reflection of some ideal calculated intensity. Unmagnetized mosaic crystal. Curves are shown for several values of $|N|/|M|$, the ratio of the nuclear to magnetic structure factor.

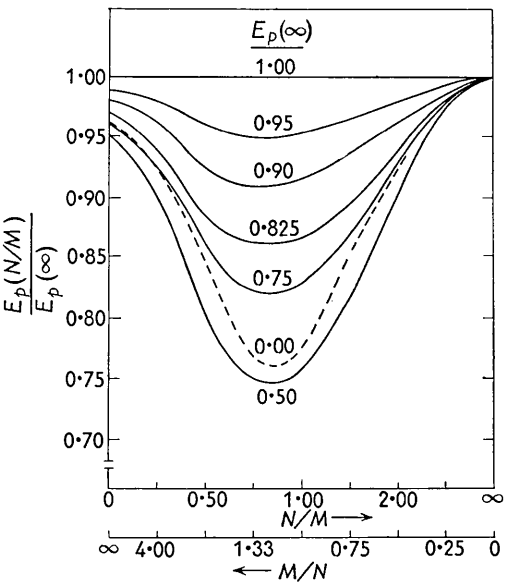

Fig. 4. $E_p(N/M)/E_p(\infty)$ versus N/M and M/N. Curves are shown for several values of $E_p(\infty)$, the extinction ratio for a pure nuclear reflection. The curves for $E_p(\infty) < 0{\cdot}5$ lie near to those for $E_p(\infty) = 0{\cdot}5$, and only the limiting curve for $E_p(\infty) = 0$ is shown (broken line). These are the same data as those in Fig. 3 plotted in another way.

There may well be some question as to the real meaning of t_0 derived in this way as there is also some question to the meaning of η in the theory of secondary extinction. Both quantities refer to ideal models which are not likely to be realized in practice, i.e., t_0 derived in this way is no more the ‚true' thickness of a mosaic block than is η the standard deviation of a real one-parameter angular distribution function. However, both quantities should have a great deal of meaning when they are compared from crystal to crystal. If η is larger, the crystal is less perfect; if t_0 is larger, the average dimensions of the scattering domains are larger.

Precession of the neutron spin

We have not yet considered one factor which will affect some of the preceding conclusions. This is the precession of the neutron spin around the magnetic axis as the neutron beam passes through the crystal.

* There may be some spread of the *nuclear* reflections from the curve due to the fact that the angle factors involved in the expressions for primary and secondary extinction differ, the exact form of the difference depending on the shape assumed for the mosaic blocks. For quantitative extinction estimates, one must be careful to take this into account, preferably by comparing intensities of reflections with approximately the same Bragg angle.

The polarization relative to **K** will of course not be affected by this precession, but since we have been discussing polarization relative to **q**, some modifications must be made. If a neutron with velocity v has an initial spin function χ_s, it will have, after having gone a distance r through a homogeneous magnetic field H, the spin function

$$\chi_s' = \left(\cos\frac{\omega r}{2v} + 2i\mathbf{K}.\mathbf{s}\sin\frac{\omega r}{2v}\right)\chi_s \tag{54}$$

with the Larmor precession frequency ω being given by

$$\omega = \gamma_n eH/M_0 c\,. \tag{55}$$

In particular, for $\chi_s \equiv \alpha$, i.e., $a = 1$, $b = 0$, we have

$$\chi_s' = \left(\cos\frac{\omega r}{2v} + iK_z\sin\frac{\omega r}{2v}\right)\alpha + \left(-K_y\sin\frac{\omega r}{2v} + iK_x\sin\frac{\omega r}{2v}\right)\beta \tag{56}$$

and thus

$$\left.\begin{aligned} |a'|^2 &= \cos^2\frac{\omega r}{2v} + K_z^2\sin^2\frac{\omega r}{2v}\,, \\ |b'|^2 &= (K_y^2+K_x^2)\sin^2\frac{\omega r}{2v}\,. \end{aligned}\right\} \tag{57}$$

Similarly, for $\chi_s \equiv \beta$, i.e., $a = 0$, $|b| = 1$, we have

$$\chi_s' = \left[(iK_x+K_y)\sin\frac{\omega r}{2v}\right]\alpha + \left[\cos\frac{\omega r}{2v} - iK_z\sin\frac{\omega r}{2v}\right]\beta \tag{58}$$

and

$$\left.\begin{aligned} |a'|^2 &= (K_y^2+K_x^2)\sin^2\frac{\omega r}{2v}\,, \\ |b'|^2 &= \cos^2\frac{\omega r}{2v} + K_z^2\sin^2\frac{\omega r}{2v}\,. \end{aligned}\right\} \tag{59}$$

We would like now to have these expressions in terms of q. Remembering that in the previous sections the **z** axis has been chosen to lie along the direction of **q**, we find

$$K_x^2+K_y^2 = 1-q^2,\quad K_z^2 = q^2\,. \tag{60}$$

Equations (57) thus become

$$\left.\begin{aligned} |a'|^2 &= \cos^2\frac{\omega r}{2v} + q^2\sin^2\frac{\omega r}{2v}\,, \\ |b'|^2 &= (1-q^2)\sin^2\frac{\omega r}{2v}\,. \end{aligned}\right\} \tag{61}$$

Equations (59) reduce to equations identical to (61) but with an interchange of $|a'|$ and $|b'|$.

Let us first examine the magnitude of this effect. For the most unfavorable case, $q^2 = 0$, the percentage change in the polarization is $\sin^2(\omega r/2v)$. If we wish the change in polarization to be less than 5%, we must have

$$\sin^2(\omega r/2v) < 0{\cdot}05,\quad (\omega r/2v) < 0{\cdot}224\,. \tag{62}$$

Now, for neutrons with a 1 Å wavelength, we find

$$(\omega r/2v) = 2{\cdot}31\times10^{-2}Hr\,. \tag{63}$$

Substituting (63) in (62), we find that

$$Hr < 10 \text{ cm. gauss} \tag{64}$$

is the necessary condition for the change in polarization to be less than 5%. For many of the experiments commonly carried out with ferromagnetic materials, H will be of the order of 10^4. The implied condition

$$r < 10^{-3} \text{ cm.} \tag{65}$$

would seem to be satisfied for the mosaic-block size in most crystals. In other words, within an individual mosaic-block, we may safely neglect the effect of the precession on the polarization and extinction. Furthermore, in an unmagnetized single crystal with random orientation of domains, there will be no net effect. The only case, then, where the conclusions of the preceding sections may need modification is the case of a magnetized single mosaic crystal.*

Let us first consider the case of no secondary extinction. The precession has no effect on the total scattered intensity; there is, however, a profound effect on the polarization of the scattered beam. If we consider a plane parallel crystal plate of thickness T, with the polarization of the scattered wave from each mosaic-block being given by P_0, the polarization of the scattered beam from the entire thickness of the crystal is given by

$$P = \frac{P_0\gamma_H}{T}\dagger\int_0^{T/\gamma_H}\cos^2\frac{\omega r}{2v} + (2q^2-1)\sin^2\frac{\omega r}{2v}\,dr = P_0\left[\frac{\sin x}{x} + q^2\left(1-\frac{\sin x}{x}\right)\right], \tag{66}$$

with

$$x = \omega T/\gamma_H V\,. \tag{67}$$

Fig. 5 shows P/P_0 as a function of x for several values of q^2. Note that this ratio approaches q^2 as x approaches infinity.

The analysis becomes more complex if secondary extinction is present. Neglecting absorption, we may write the power equations for symmetrical diffraction from infinite flat plates as follows:‡

$$\frac{d\mathscr{P}_0^+}{dt} = -\sigma^+(\mathscr{P}_0^+-\mathscr{P}_H^+)\left[1-B\sin^2\frac{\omega t}{2v\gamma}\right] - \sigma^-(\mathscr{P}_0^--\mathscr{P}_H^-)B\sin^2\frac{\omega t}{2v\gamma} - (2\alpha-1)\frac{\omega B}{2v\gamma}\sin\frac{\omega t}{v\gamma}\,, \tag{68}$$

* Large domains in crystals with no net magnetization are included in this description.

† γ here and in the following is the direction cosine of the scattered wave, *not* the neutron spin.

‡ B is defined as $1-q^2$. $\mathscr{P}_H$ and $\mathscr{P}_0$ are the powers of the diffracted and incident beams, the superscripts referring to the polarization directions. σ is defined in (45) and (46). $2\alpha-1$ is the initial polarization.

$$\frac{d\mathscr{P}_H^+}{dt}(\text{Bragg}) = -\sigma^+(\mathscr{P}_0^+ - \mathscr{P}_H^+)\left[1 - B\sin^2\frac{\omega(T-t)}{2v\gamma}\right] - \sigma^-(\mathscr{P}_0^- - \mathscr{P}_H^-)B\sin^2\frac{\omega(T-t)}{2v\gamma}, \quad (69)$$

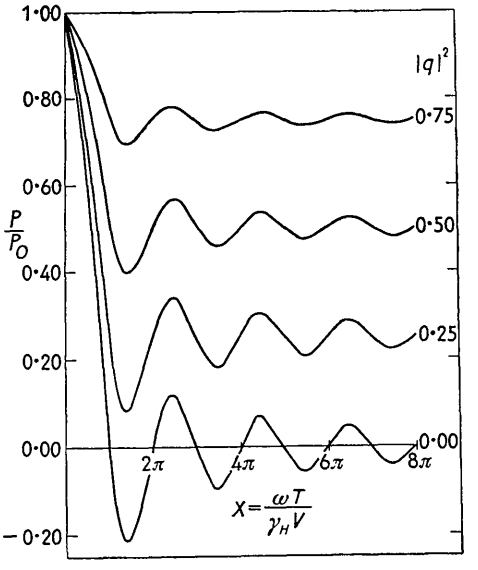

Fig. 5. Depolarization of scattered wave due to precession of neutron spin in magnetized flat-plate mosaic crystal which exhibits no secondary extinction. Curves give ratio of final polarization (P) to polarization (P_0) defined by the scattering from the individual mosaic blocks. Abscissa is $x = \omega T/\gamma_H v$. The curves, which are given for several values of q^2, fluctuate about a limiting value of q^2.

$$\frac{d\mathscr{P}_H^+}{dt}(\text{Laue}) = \sigma^+(\mathscr{P}_0^+ - \mathscr{P}_H^+)\left(1 - B\sin^2\frac{\omega t}{2v\gamma}\right) + \sigma^-(\mathscr{P}_0^- - \mathscr{P}_H^-)B\sin^2\frac{\omega t}{2v\gamma}, \quad (70)$$

with analogous equations for $\mathscr{P}_0^-$ and $\mathscr{P}_H^-$. The solution of these equations is tedious, and a detailed discussion will be reserved for a future paper. Only the results for one particular simple example will be presented here to indicate that the effects are not trivial. For the Laue case with $\alpha = \frac{1}{2}$, $\sigma^- = 0$, we obtain

$$\frac{\mathscr{P}_H^+ + \mathscr{P}_H^-}{\mathscr{P}_0^+(0) + \mathscr{P}_0^-(0)} = \frac{\sigma^+ T}{2}\int_0^1 \exp\left[2\sigma^+ T\xi\left(\frac{B}{2}\left\{1 - \frac{\sin x\xi}{x\xi}\right\} - 1\right)\right]d\xi. \quad (71)$$

The value of this function for $B = 1$* normalized to unity for $x = 0$ is plotted in Fig. 6 as a function of $x = \omega T/v\gamma$ for several values of $\sigma^+ T$. Note that the general effect is an enhancement of intensity over that to be expected for $x = 0$. In certain situations, a variation of intensity as a function of x may be observed. The period of this variation may be used to estimate the internal field in the crystal. In interpreting any experiment, of course, one must be careful to take into consideration any magnetic saturation curve that might be applicable to the particular situation.

* This does not correspond to a real physical situation, as it is impossible for σ^- and q to both be equal to zero. The general behavior is the same, however, for other values of B.

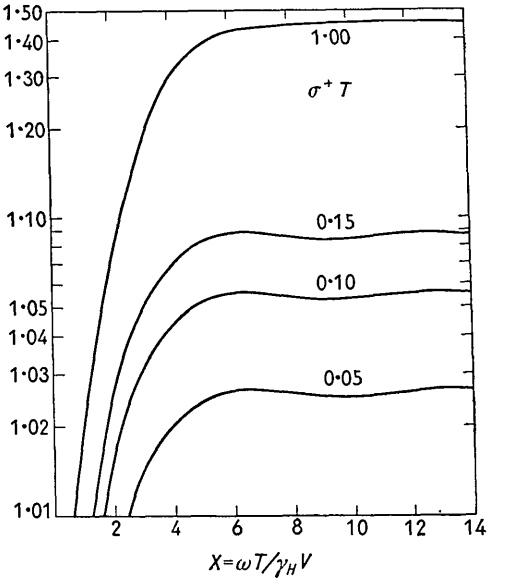

Fig. 6. Solutions of equation (71) for $B = 1$. Each curve is normalized to unity for $x = 0$.

Summary

1. In an unmagnetized mosaic crystal, more severe extinction for reflections with magnetic contributions can only be due to primary extinction. One can thus easily determine relative amounts of primary and secondary extinction.

2. In a magnetized mosaic crystal, both primary and secondary extinction are more severe for mixed nuclear–magnetic reflections. If extinction is severe, precession of the neutron spin may be important in determining the intensity.

3. Total extinction effects for a particular crystal model may be calculated in the following way:

(*a*) Substitute $|F_+|$ and $|F_-|$ into (27) or corresponding equation for the Laue case to obtain R_+^θ and R_-^θ for a single mosaic-block. Make this calculation for every value of **q** if a multi-domain mosaic crystal is to be treated.

(*b*) For a magnetized mosaic crystal (or a single domain in an unmagnetized crystal if secondary extinction within the domain is likely to be severe), use R_+^θ and R_-^θ from (*a*) to calculate $(E_p)_+$ and $(E_p)_-$ and consequently σ_+'' and σ_-''. Carry out secondary-extinction calculations for each of these separately and add final integrated intensities.

(*c*) For an unmagnetized crystal with small random domains, average R^{θ}_{+} or R^{θ}_{-} from (*a*) over all values of $\mathbf{q}$ to obtain an average $\overline{R^{\theta}}$ for the individual mosaic blocks. Use this $\overline{R^{\theta}}$ and resulting $\overline{E_p}$ to define σ'' as in (40–41) and proceed to make a single secondary extinction calculation for the entire crystal.

Many of the results developed in this paper have been experimentally verified by the author on the single crystal of magnetite previously mentioned and by polarized beam experiments carried out by Dr C. G. Shull and Dr Robert Nathans (private communication). Details of the applications of this paper will be given in forth-coming papers dealing with the individual experiments. The author would like to express his appreciation to Dr Nathans, Dr L. M. Corliss, and Dr J. M. Hastings for helpful discussions and to Mr David Langdon for assistance in carrying out the numerical calculations.

APPENDIX

The scattered wave function for a structure composed of several magnetic ions may be written

$$\psi_H = (2\pi M_0/hk)^{\frac{1}{2}} r^{-1} \exp[ikr] \left[\sum_j b_j \exp[i\mathbf{r}_j.\mathbf{h}] + 2\sum_j p_j \mathbf{q}_j.\mathbf{s} \exp[i\mathbf{r}_j.\mathbf{h}]\right]\chi_s , \quad (72)$$

and the scattering cross-section for an incident wave with polarization direction $\boldsymbol{\lambda}$ may be written

$$\sigma_\lambda = N^2 + 2N\sum_j p_j \mathbf{q}_j.\boldsymbol{\lambda} \exp[i\mathbf{r}_j.\mathbf{h}] + \sum_j \sum_k p_j p_k \mathbf{q}_j.\mathbf{q}_k \exp[i(\mathbf{r}_j - \mathbf{r}_k).\mathbf{h}] \quad (73)$$

with the nuclear structure factor defined as

$$N \equiv \sum_j b_j \exp[i\mathbf{r}_j.\mathbf{h}] . \quad (74)$$

Clearly, if all the $\mathbf{q}_j$ are parallel or antiparallel and of the same magnitude

$$\mathbf{q}_j = \pm\mathbf{q} , \quad (75)$$

we may write

$$\sigma_\lambda = N^2 + 2NM\mathbf{q}.\boldsymbol{\lambda} + q^2M^2 \quad (76)$$

if the magnetic structure factor M is defined as

$$M = \sum_j \pm p_j \exp[i\mathbf{r}_j.\mathbf{h}] \quad (77)$$

with the + or − sign chosen according as $\mathbf{q}_j$ is parallel or antiparallel to $\mathbf{q}$. If (75) and (76) are valid, then all the equations for a complete structure may be obtained from those for a single ion by replacing b and p by N and M. It is interesting to compare the expressions for the cross-sections derived from (73) and (76) for the case of a random orientation of domains with respect to the scattering vector. We find that (76) reduces to

$$\sigma = N^2 + (\tfrac{2}{3})M^2 ,$$

while (73) for the general case reduces to

$$\sigma = N^2 + (\tfrac{2}{3})\sum_j \sum_k p_j p_k \cos\beta_{jk} \exp[i(\mathbf{r}_j - \mathbf{r}_k).\mathbf{h}] , \quad (78)$$

where β_{jk} is the angle between $\mathbf{K}_j$ and $\mathbf{K}_k$.

In our treatment of primary extinction, we have required that the spin be analyzed along a unique axis chosen so that no spin flip due to scattering occurs:

$$(\alpha|\mathbf{q}.\mathbf{s}|\beta)^2 = 0 . \quad (79)$$

The condition corresponding to (79) for the general case of non-parallel spins is

$$\left[\sum_j p_j(\alpha|\mathbf{q}_j.\mathbf{s}|\beta) \exp[i\mathbf{r}_j.\mathbf{h})]\right]^2 = 0$$

or

$$\left[\sum_j p_j(q_j)_x \exp[i\mathbf{r}_j.\mathbf{h}]\right]^2 + \left[\sum_j p_j(q_j)_y \exp[i\mathbf{r}_j.\mathbf{h}]\right]^2 = 0 \quad (80)$$

since

$$(\alpha|\mathbf{q}.\mathbf{s}|\beta) = \tfrac{1}{2}(q_x - iq_y) . \quad (81)$$

We may set the second term in (80) equal to zero merely by choosing the $\mathbf{y}$ axis to be parallel to $\boldsymbol{\epsilon}$, and the $\mathbf{x}$ and $\mathbf{z}$ axes consequently in the scattering plane, which also contains all the $\mathbf{q}_j$. Thus we must find an axis in the plane such that the first term in (80) vanishes. This implies that both the following conditions be satisfied:

$$\sum_j p_j(q_j)_x \cos(\mathbf{r}_j.\mathbf{h}) = 0 , \quad (82)$$

$$\sum_j p_j(q_j)_x \sin(\mathbf{r}_j.\mathbf{h}) = 0 . \quad (83)$$

Both these equations can in general be satisfied only if the magnetic structure is *centrosymmetric*,* in which case (83) is satisfied because of the symmetry. A unique $\mathbf{x}$ axis in the plane can then be found which causes (82) to be satisfied. If $(q_j)_{x'}$ and $(q_j)_{z'}$ are the components of $\mathbf{q}_j$ relative to an arbitrary set of axes $\mathbf{x}'$ and $\mathbf{z}'$, a new set of axes $\mathbf{x}$ and $\mathbf{z}$ given by

$$\mathbf{x} = \mathbf{x}'\cos\theta + \mathbf{z}'\sin\theta, \quad \mathbf{z} = -\mathbf{x}'\sin\theta + \mathbf{z}'\cos\theta \quad (84)$$

will cause (82) to be satisfied if

$$\tan\theta = -\frac{\sum_j p_j(q_j)_{x'} \cos(\mathbf{r}_j.\mathbf{h})}{\sum_j p_j(q_j)_{z'} \cos(\mathbf{r}_j.\mathbf{h})} . \quad (85)$$

Equation (73) then becomes

* This does *not* mean that the spin is reversed through inversion at the origin, but rather that on inversion one obtains an identical atom with the spin in the same direction. The magnetic structures of simple ferromagnetic and antiferromagnetic compounds are generally centrosymmetric; indeed most of them would seem to satisfy the more stringent requirement of having parallel and anti-parallel spins.

$$\sigma_z = N^2+2N\sum_j p_j(q_j)_z \cos(\mathbf{r}_j.\mathbf{h}) + \sum_j\sum_k p_j p_k (q_j)_z (q_k)_z \cos[(\mathbf{r}_j-\mathbf{r}_k).\mathbf{h}], \quad (86)$$

or

$$\sigma_z^{1/2} = |F_z| = N+\sum_j p_j(q_j)_z \cos(\mathbf{r}_j.\mathbf{h}), \quad (87)$$

with $(q_j)_z$ being the **z** component of $\mathbf{q}_j$ relative to the new set of axes:

$$(q_j)_z = -(q_j)_{x'} \sin\theta + (q_j)_{z'} \cos\theta . \quad (88)$$

In all of the previous discussion in this paper, we may then make the formal substitution

$$M|q| = \sum_j p_j(q_j)_z \cos(\mathbf{r}_j.\mathbf{h}) . \quad (89)$$

References

CHANDRASEKHAR, S. & WEISS, R. J. (1957). *Acta Cryst.* **10**, 598.

GOLDBERGER, M. L. & SEITZ, F. (1947). *Phys. Rev.* **71**, 294.

HALPERN, O. & JOHNSON, M. H. (1939). *Phys. Rev.* **55**, 898.

HAMILTON, W. C. (1957). *Acta Cryst.* **10**, 629.

ZACHARIASEN, W. H. (1945). *Theory of X-ray Diffraction in Crystals*. New York: Wiley.

Acta Cryst. (1958). **11**, 594

The Structure of Roussin's Black Salt, $CsFe_4S_3(NO)_7.H_2O$

BY GEORG JOHANSSON AND WILLIAM N. LIPSCOMB

School of Chemistry, University of Minnesota, Minneapolis 14, *Minnesota, U.S.A.*

(*Received* 31 *October* 1957)

The structure of the Roussinate ion, $Fe_4S_3(NO)_7^-$, has been determined from the Cs^+ and K^+ salts. The unit-cell parameters of the Cs^+ salt are

$$a = 9{\cdot}5_9,\ b = 9{\cdot}7_8,\ c = 10{\cdot}1_2 \text{ Å},\ \alpha = 112{\cdot}8°,\ \beta = 103{\cdot}5°,\ \gamma = 96{\cdot}5°;$$

and the space group is $P\bar{1}$. The isolated ion has approximately C_{3v} symmetry, with a tetrahedral arrangement of Fe, and 3 S above the centers of three faces. All FeNO groups are roughly linear, and no NO bridges occur. Average distances are Fe_I(apex) $\cdots$ Fe_{II} = 2·70 Å, $Fe_{II} \cdots Fe_{II}$ = 3·57 Å, Fe–S = 2·23 Å, $Fe_I{\equiv}N$ = 1·57 Å, $Fe_{II}{=}N$ = 1·67 Å, N=O = 1·20 Å. Our preferred electronic structure has 4 non-bonding electrons on each Fe, and one electron pair in a highly delocalized molecular orbital among the 4 Fe atoms, thus accounting for the diamagnetism and the high absorption coefficient.

Introduction

A prerequisite to any valence theory of the black Roussinate ion $Fe_4S_3(NO)_7^-$ is its structure determination, reported here. The chemical evidence for various proposed structures has been summarized by Addison & Lewis (1955), who list Seel's (1942) proposal based on the FeS structure and on Manchot & Linckh's (1926) early proposal of the $\{[(NO)_2FeS]_3Fe(NO)\}^-$ formula; but Addison & Lewis, as well as earlier authors, have proposed similar structures in which NO bridges occur. None of the electronic interpretations of these proposed structures have accounted for the observed diamagnetism (Cambi & Szegö, 1931). It seems probable that the electronic interactions giving rise to this diamagnetism are sufficiently weak to account also for the intense transitions to low-lying electronic levels which are indicated by the high extinction coefficient of this ion. A preliminary discussion of the valence structure is therefore included as a part of this structure determination by the X-ray diffraction method.

Experimental procedure

The K salt and Na salt were prepared from $NaNO_2$, KHS ($KOH+H_2S$) and $FeSO_4$ by the method of Pawel (1882). The Cs salt was obtained by the addition of Cs_2SO_4 to a solution of the Na salt.

A crystal of the Cs salt having dimensions 0·15×0·15×0·05 mm. was photographed with Mo $K\alpha$ radiation at a precession angle of 25° in the Buerger. Although the linear absorption coefficient is 62 cm.$^{-1}$, no corrections for absorption or extinction were made. The 1443 observed reflections were obtained from the $h0l$; $h1l$; $h2l$; $h3l$; $h4l$; $0kl$; $1kl$; $2kl$; $3kl$; $4kl$; $2h,\bar{h},l$; $2h+1,\bar{h},l$; $h,\bar{h},l$; $h-1,\bar{h},l$; $h,2\bar{h},l$; $h,2h,l$; hhl, $h+1,h,l$; and $h+2,h,l$ reciprocal lattice planes. For the K salt, a total of 200 $h0l$ and $0kl$ reflections were estimated.

The crystals were triclinic with cell parameters